

Ultra-compact silicon nanophotonic modulator with broadband response

Volker J. Sorger¹, Norberto D. Lanzillotti-Kimura¹, Ren-Min Ma¹ and Xiang Zhang^{1,2,*}

¹NSF Nanoscale Science and Engineering Center, 3112 Etcheverry Hall, University of California, Berkeley, CA 94720, USA

²Materials Sciences Division, Lawrence Berkeley National Laboratory, 1 Cyclotron Road, Berkeley, CA 94720, USA, e-mail: Xiang Zhang: xiang@berkeley.edu

*Corresponding author

Abstract

Electro-optic modulators have been identified as the key drivers for optical communication and signal processing. With an ongoing miniaturization of photonic circuitries, an outstanding aim is to demonstrate an on-chip, ultra-compact, electro-optic modulator without sacrificing bandwidth and modulation strength. While silicon-based electro-optic modulators have been demonstrated, they require large device footprints of the order of millimeters as a result of weak non-linear electro-optical properties. The modulation strength can be increased by deploying a high-Q resonator, however with the trade-off of significantly sacrificing bandwidth. Furthermore, design challenges and temperature tuning limit the deployment of such resonance-based modulators. Recently, novel materials like graphene have been investigated for electro-optic modulation applications with a 0.1 dB per micrometer modulation strength, while showing an improvement over pure silicon devices, this design still requires device lengths of tens of micrometers due to the inefficient overlap between the thin graphene layer, and the optical mode of the silicon waveguide. Here we experimentally demonstrate an ultra-compact, silicon-based, electro-optic modulator with a record-high 1 dB per micrometer extinction ratio over a wide bandwidth range of 1 μm in ambient conditions. The device is based on a plasmonic metal-oxide-semiconductor (MOS) waveguide, which efficiently concentrates the optical modes' electric field into a nanometer thin region comprised of an absorption coefficient-tuneable indium-tin-oxide (ITO) layer. The modulation mechanism originates from electrically changing the free carrier concentration of the ITO layer which dramatically increases the loss of this MOS mode. The seamless integration of such a strong optical beam modulation into an existing silicon-on-insulator platform bears significant potential towards broadband, compact and efficient communication links and circuits.

Keywords: Modulator; silicon-on-insulator; ultra-compact.

A waveguide-integrated electro-optical modulator can be perceived as a transistor with an optical source and drain and an electrical gate [1]. This waveguide receiving a continuous wave laser beam converts electrical data arriving at the gate electrode into an optical encoded data stream. A widely used modulation mechanism is to change the free carrier concentration of the material overlapping with the propagating optical mode, which leads to a shift of the plasma frequency of the dispersion relation [2]. This modifies both the real and imaginary parts of the refractive index of the material, and henceforth alters the index and loss of the optical propagating mode. While a Mach-Zehnder type modulator utilized a refractive index change in the real part [3], an electro-absorption type modulator deploys the altered loss of the optical mode [4]. With the promise of silicon-on-insulator (SOI) technology [5] for on-chip integrated photonics, the Intel team demonstrated a Mach-Zehnder modulator by changing the real part of silicon refractive index [3]. However, a large device footprint up to several millimeters in size is required to obtain sufficient extinction ratios owing to the limited carrier modulating effect of silicon [2, 3]. Shrinking the footprint was successfully achieved by deploying an SOI resonator design incorporating a high quality factor cavity which can boost the weak index-changing modulation effect [6]. The high extinction ratios obtained were compromised, however, by the minuscule bandwidth (<0.1 nm) over which the modulation can be pertained. Thus, resonator-based electro-optic modulators require painstaking fabrication tolerances of the high-Q cavity and are temperature-prone calling for sophisticated athermal designs and operation requirements [6]. Both the footprint and bandwidth constrains can be simultaneously overcome by (i) enhancing the optical mode overlap with the actively index-modulated region (geometric effect) [7–9], and (ii) increasing the light-matter-interaction of the optical mode with the actively index-modulated material via enhancing the electromagnetic-field strength (absorptive effect) [9–11]. We achieve both of these desired effects by deploying a plasmonic metal-oxide-semiconductor (MOS) type optical mode which concentrates part of the propagating mode's field into a nanometer-thin region overlapping with the actively index-modulated material [7–9]. Note, that the in the SOI remaining part of the optical mode ensures a low impedance mismatch to the SOI waveguide portion, allowing for a waveguide-integrated design with low insertion loss. The active material responsible for the modulation is a nanometer thin

indium-tin-oxide (ITO) layer inside the MOS mode. ITO belongs to the class of transparent conducting oxides which can be doped depending on the oxygen vacancy and interstitial metal dopant concentrations [12, 13]. Furthermore, the carrier density can be greatly increased when ITO becomes part of a MOS-capacitor design upon applying an electrical bias, due to the formation of an accumulation layer increasing the index-modulation strength of the optical mode [14, 15].

Here we report an ultra-compact, waveguide-integrated, nanophotonic electroabsorption modulator by actively tuning the ITO carrier density inside a MOS-type structure. The device features an extinction ratio as high as $1 \text{ dB } \mu\text{m}^{-1}$ and a broadband operation spanning a wavelength range of $1.2\text{--}2.2 \text{ } \mu\text{m}$ with a relatively low insertion loss of about -1 dB for a $5 \text{ } \mu\text{m}$ long device. In addition, this modulator is constructed using the silicon-on-insulator platform making it compatible with current silicon photonics technology.

The ultra-compact nanophotonic modulator comprises a silicon strip waveguide and a metallic gold pad with a gate oxide (SiO_2 , $t_{\text{ox}}=20 \text{ nm}$) and an active ITO layer ($t_{\text{ITO}}=10 \text{ nm}$) sandwiched between them (Figure 1A). The gate stack (ITO-SiO₂-Au) is placed on top of the SOI waveguide via electron-beam lithography, electron-beam evaporation and lift off processing (Figure 1B). In order to study the modulation response, a continuous wave laser beam at telecom wavelengths is free-space coupled into and out of the SOI waveguide via grating couplers as shown in Figure 1B, while a voltage bias across the MOS capacitor leads to the MOS-mode's index change altering the laser beams intensity. A key design criterion is to place ITO layer with the active tuneable absorption coefficient in the center of the MOS mode where the electric field presents its maximum (Figure 1C). The electromagnetic wave propagating in such a four-layer structure is a hybrid plasmonic MOS mode which offers a unique combination of both strong optical confinement significantly below the diffraction limit of light and relatively low wave propagation loss [7–9]. The confinement stems from a continuity of the displacement field, D , at the material interfaces leading to a strong electric field in the thin oxide layer normal to the metal and the semiconductor, as well as from a built-up polarization charge creating an optical capacitor confining the electromagnetic field energy [7].

The performance of this nanophotonic modulator of various lengths shows an extinction ratio of 5 dB and more than 20 dB for device lengths of 5 and $20 \text{ } \mu\text{m}$, respectively, when a voltage bias between the silicon (ground) and metal (positive) contact is applied (Figure 2A). These results correspond to an extinction ratio of $1 \text{ dB}/\mu\text{m}$ which is, to the best of our knowledge, the highest value among all the reported Si-based electro-optic modulators [3, 4]. The high performance of the devices is a direct result of both the strong optical confinement of the MOS mode [7–9] and the ITO's capability to change its optical refractive index and loss under electrical bias [14]. Placing the ITO layer between the metal and the semiconductor where the electromagnetic field presents its maximum strongly enhances the modulation effect due to the increased electro-optic absorption of the optical mode. Noteworthy is also the low voltage required to switch the signal off; while

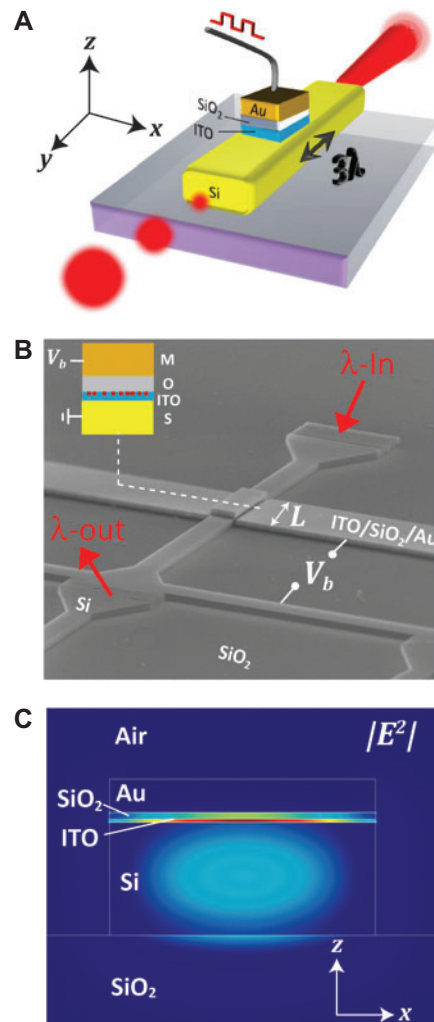


Figure 1 (A) Schematic of the ultra-compact, waveguide-integrated, silicon-based nanophotonic modulator. The device length is just a few wavelengths long (not to scale). Electrical data become encoded on an optical beam via the electroabsorption effect. The MOS design features a plasmonic optical mode which concentrates the mode's electric field and allows for a good overlap with the active ITO layer; in short gives rise to enhanced light-matter-interactions. (B) Scanning electron micrograph of a finished device MOS section length, $L=5 \text{ } \mu\text{m}$. A continuous wave laser was free space coupled into the SOI waveguide via grating couplers which were designed to operate at $\lambda = 1310 \text{ nm}$ and had a pitch of pitch of 590 nm , a silicon slap length of 210 nm . They were fabricated with electron-beam lithography and reactive-ion-etching using chromium as a hard etch mask, which was finally removed with a wet etch step (CR-7). The MOS stack (ITO-SiO₂-Au) was placed on top the SOI waveguide with an aligned second lithography step and electron beam evaporation. Inset: Schematic of the modulator crosssection illustrating the operating mechanism principle; when an electrical voltage bias is applied across this MOS capacitor an accumulation layer is formed at the ITO-SiO₂ interface, increasing the ITO's carrier density which increases the imaginary part of the refractive index, κ , leading an increased MOS mode loss. (C) Electric field density across the active fundamental MOS region of the modulator showing the maximum of the MOS modes' field intensity coinciding with the active ITO layer (FEM simulation). Material parameters: $\bar{n}_{\text{Si}}=3.541-0.0001i$, $\bar{n}_{\text{ITO}}=1.042-0.273i$, $n_{\text{SiO}_2}=1.45$, $\bar{n}_{\text{Air}}=0.31-9.00i$ at $\lambda=1310 \text{ nm}$ (see Figure 3 and supplementary online material).

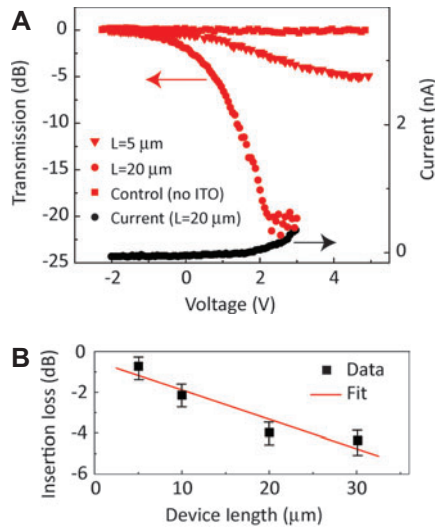


Figure 2 (A) The modulator performance yields a record-high 1 dB/ μm extinction ratio and is a direct result of the plasmonic MOS mode and the active’s material (ITO) ability to alter its optical loss. Increasing the device length, L , results in stronger modulation down to -20 dB for a 20 μm long device. The voltage polarity was chosen such that the gold contact was forward biased (positive pole) with the silicon being grounded. No modulation was observed for reversed bias polarity and when the ITO layer was omitted in the device (black squares). The MOS capacitor operation is indirectly verified by a low leakage current of about half a nano-ampere for an applied bias of 3 volts (red circles). (B) The total insertion loss comprising of both the SOI-to-MOS coupling (-0.25 dB/coupler) and plasmonic MOS mode propagation (-0.14 dB/ μm) were estimated by the cut-back method. For a 5 μm long modulator the total insertion loss is only about -1 dB due to the good impedance match between the SOI and MOS mode and low ohmic losses from the plasmonic MOS mode [7–9].

dielectric modulators show index changes per applied voltages of only one millionth, the modulator studied here has a 10,000 times stronger voltage modulation potential, for similar electrostatics geometries (Figure 2A) [3]. In our control samples where the ITO layer is omitted no beam modulation was observed even for longer devices of up to 30 μm in length (Figure 2A). Notice that the leakage current levels of the MOS capacitor are very low (<0.5 nA), suggesting a good capacitive coupling and successful formation of the MOS accumulation layer (Figure 2A). Further control tests support that the leakage current decreases with the increasing oxide thickness suggesting the proper operation of the MOS capacitor (see supplementary online material).

An important device and photonic circuit design criterion is the insertion loss in the ON-state (no voltage applied) of the electro-optic modulator, where the goal is to minimize the optical loss. Our device has two insertion loss mechanisms; one originating from the Si-to-MOS-mode impedance mismatch and another from the plasmonic metal losses of the propagating MOS-mode inside the modulator. In order to reduce the optical coupling losses from the Si-to-MOS-mode we adapted a thick silicon waveguide (width = 800 nm, height = 340 nm) such that a portion of the optical mode resides

in the silicon core reducing the impedance mismatch between the two waveguide sections. This silicon waveguide thickness also allows a large amount of the electromagnetic wave to propagate in the low loss Si region, which minimizes the plasmonic MOS mode metal losses. Furthermore, the doping level of the silicon was chosen to be reasonably low ($5 \times 10^{17} \text{ cm}^{-3}$) in order to reduce optical losses. By deploying the cut-back method, we can separate these two loss mechanisms and found about half a dB originating from coupling twice between the Si-MOS sections, and about -0.1 dB/ μm propagation loss of the MOS-mode with the latter corresponding to a propagation length of 43 μm (Figure 2B). Thus, a 5 μm long device suffers a total insertion loss of only about 1 dB. Towards verifying the coupling loss (SOI-to-MOS) we performed numerical simulations using the commercial package COMSOL. We calculated the modal indices from the eigenmode solver and found the reflection coefficient from the modal impedance mismatch between the SOI and the MOS sections to be about 1% (see below for details). However, additional scattering from the gate-stack corners can be attributed to make up for the measured -0.25 dB per coupler. This overall low loss is a significant improvement over dielectric modulators which require millimeter long interaction lengths [3]; thus even if their modal loss is much lower than that of the plasmonic MOS mode, smallest line-etch roughness imperfections accumulate over millimeter long distances.

The observed high performances of the devices have been verified in numerical simulations. The Drude-Lorentz model has been used for describing the permittivity of ITO and its index-altering behavior as a function of the carrier concentration, i.e., under electrical bias (see supplementary online material) [14–16]. In order to use this model for the numerical device simulations we need to find the ITO carrier densities corresponding to the ON (no voltage) and OFF (voltage applied) states, which we obtained consecutively; experimental four-probe measurements of the ITO film yield a ON-state value of the sheet resistance of $R_{sq} = 4708 \Omega/sq$, and with the film thickness of 80 nm a resistivity of $\rho = R_{sq} t_{ITO} = 0.038 \Omega\text{cm}$ corresponding to an ON-state carrier density of $(n_c - ITO)_{ON} = 1.1 \times 10^{19} \text{ cm}^{-3}$. In order to simulate the OFF-state of the modulator, we use a 2D analytical model describing the dispersion relation across the MOS-stack. Using this approach we can find the carrier density of the ITO film for the OFF state, from which we obtain the material parameters, n and κ via the Drude-Lorentz model. These results are summarized in the table of Figure 3A which correspond to a change in the carrier density of $6.7 \times 10^{20} \text{ cm}^{-3}$ between the ON and OFF states and an increased plasma frequency of the ITO changing from being a dielectric to becoming quasi metallic in the ON and OFF states, respectively. Using these data, we numerically simulated the electric field distribution of the plasmonic MOS mode and overlaid the electric field density across the MOS-stack to find the peak of the electric field density inside the MOS mode to coincide with the active ITO layer (Figure 3B). Furthermore, the applied bias forms an accumulation layer at the ITO-SiO₂ interface which significantly increases the ITO’s imaginary part of the refractive index and constitutes the physical origin of the modulation mechanism

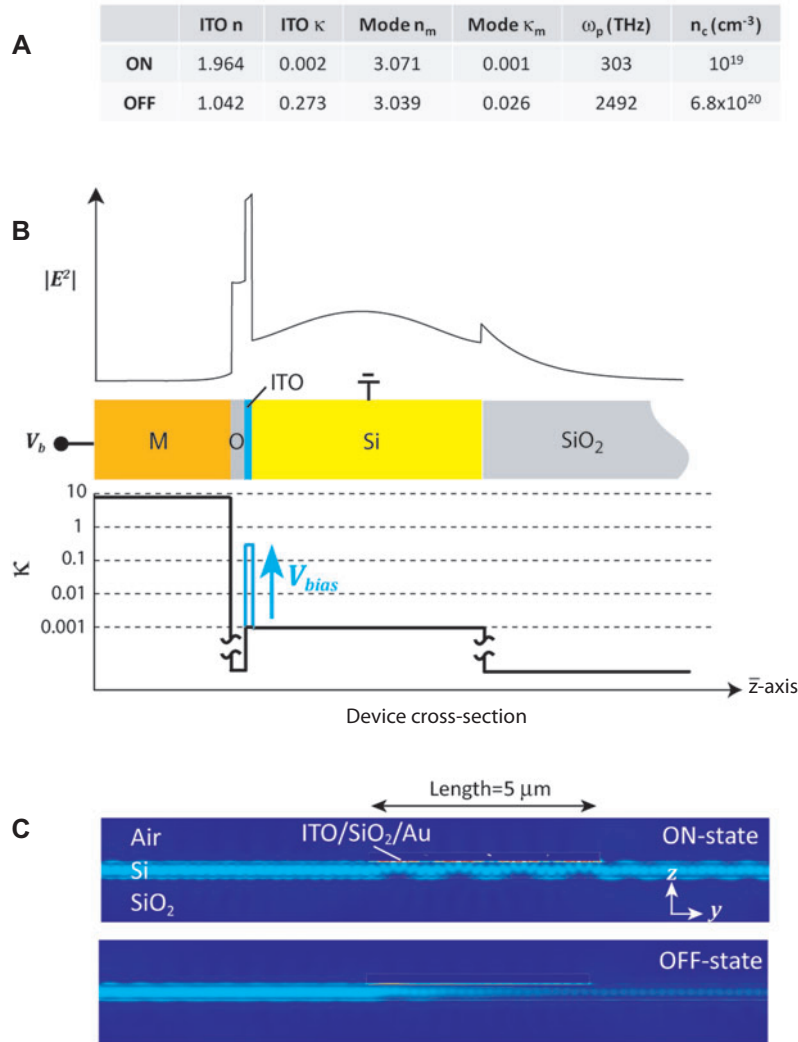


Figure 3 (A) Material and mode index summary from the applied Drude-Lorentz model in combination with experimental measured parameters and an analytical model. The results show a significant ITO and MOS modal loss, κ , increase corresponding to a significant raise of the ITO's carrier density of about 60 times. (B) The peak of the electric field density across the fundamental MOS mode coincides with the area of the active ITO layer resulting in strong absorption in the modulator OFF-state (upper panel). Under voltage bias the carrier density change inside the ITO layer results in an increased imaginary part of the refractive index of the ITO layer by more than two orders of magnitude due to the formation of an accumulation layer in the MOS capacitor (lower panel). (C) Finite-element-method simulation results of a $5 \mu\text{m}$ long modulator. A mode matched beam is launched from the left into the SOI waveguide and the time averaged power-flow across the SOI-boundary on the right recorded resulting in an extinction ratio of -4.8 dB which is in good agreement with the experimental performance from Figure 2A. The structure supports two MOS modes which beat with each other (see Supplementary online information). $\lambda = 1310 \text{ nm}$, material parameters: $\tilde{n}_{\text{Si}} = 3.541 - 0.0001i$, $n_{\text{SiO}_2} = 1.45$, $\tilde{n}_{\text{Au}} = 0.31 - 9.00i$. ITO parameters from the table in panel A.

(Figure 3B and supplementary online material). The lower panel of Figure 3 highlights the change of the imaginary part of the refractive index of the materials across the MOS-capacitor upon applying a voltage bias, namely the increased ITO loss.

We further performed 2D transmission simulations using the results from the table in Figure 3A, where we inserted the ITO material index parameters for the ON and OFF states. In the simulation, we launched a mode-matched light beam from the left into the silicon waveguide and monitored the power-flow through the silicon boundary on the right

(Figure 3C). The resulting transmission changes are -4.8 dB and -19.1 dB for the $5 \mu\text{m}$ and $20 \mu\text{m}$ long modulators, respectively, and are in good agreement with the experimental values from Figure 2A. In the ON-state one notices a variation in the power flow in the MOS section originating from two transverse magnetic (TM) MOS modes (z -direction) beating owing to the 340 nm thick silicon core. When the ITO is quasi metallic (OFF-state) the higher order TM mode, which has a second maximum close to the silicon-ITO interface, becomes more attenuated and hence the beating effect is suppressed, while the inverse occurs in the ON-state. The coupling length

from the SOI waveguide section into the MOS mode is about 0.4λ suggesting the possibility to design sub- λ long electroabsorption modulators with reasonable extinction ratio performances. Summarizing, the simulation results yield the ITO film to change from being dielectric ($n_{ITO} > 1$) to quasi-metallic ($n_{ITO} \sim 1$) which effectively increases the optical field intensity in the ITO section as a result of a stronger discontinuity of the displacement current across the MOS-stack [7]. Simultaneously the increased carrier density leads to an increased loss which facilitates absorption of the laser light in the OFF-state. The real part of the MOS modal index is only marginally altered supporting the observed low insertion loss from the small impedance mismatch between the silicon and the MOS waveguide section. From the modal loss, a_m , we can estimate the incurred laser beam transmission change, T/T_0 , for a given device length according to $T(L) = T_0 \exp(-\alpha L)$, where $\alpha = 4\pi k_m / \lambda$, k_m is the modal imaginary part of the refractive index, and λ the operating wavelength. For a modulator length of $L = 5$ and $20 \mu\text{m}$, we obtain -5.1 dB and -20.3 dB, which is in good agreement with the observed values from Figure 2A.

In telecommunications the scheme of wavelength-division-multiplexing (WDM) has itself established as the means of delivering high data bandwidths [17], which demands a broadband operation of on-chip electro-optic modulation or carefully designed resonator structures. We experimentally tested the broadband response of this modulator by scanning the operating wavelength from 1.2 to $2.2 \mu\text{m}$ and measuring the relative transmission as a function of voltage (Figure 4). The modulator showed good performance over this $1 \mu\text{m}$ bandwidth. We note that this performance could be extended by replacing the free space grating couplers with optical fiber coupling. The results from Figure 4 also show an optimum extinction ratio around a wavelength of 1600 nm. This experimental result could be explained with the findings from the Drude-Lorentz model for the ITO film (see supplementary online material); as the wavelength increases from 1.3 to $1.6 \mu\text{m}$ the change between the two carrier densities (ON-to-OFF

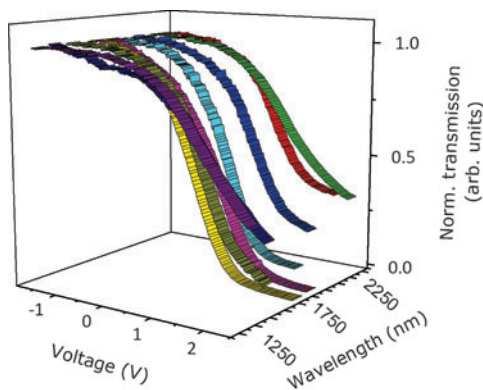


Figure 4 Broadband operation from 1.2 to $2.2 \mu\text{m}$ is possible due to the underlying non-resonant MOS mode indicating potential in WDM applications. A Ti:Sapphire femtosecond-laser in combination with an optical-parametric-oscillator was free-space coupled into the SOI grating couplers. $L = 20 \mu\text{m}$.

state) increases with a maximum around $1.6 \mu\text{m}$, after which it starts to drop. A stronger index (real part) change means more optical field is pulled into the strong absorptive ITO region. At the same time the losses increase with increasing wavelength, thus enhancing the effect. After $1.6 \mu\text{m}$ the losses still continue to increase, but the index change is reduced significantly. The Drude-Lorentz model predicts that for wavelengths beyond $4 \mu\text{m}$ an increased carrier concentration does not lower, but rises the ITO index, hence significantly more field is pushed away from the ITO region into the lower index silicon oxide layer in the OFF-state. However, as it stands, this broadband high performing modulation behavior is a direct result of the underlying non-resonant MOS mode and presents promise for future deployment into WDM on-chip architectures.

Summarizing these results, the ultra-compact footprint, high extinction ratio per device length, low insertion loss and broadband operation of this nanophotonic modulator are a result of the underlying plasmonic MOS mode: (1) inserting the active material exactly where the MOS mode has its maximum electromagnetic field strongly enhances the modulation effect. (2) The plasmonic MOS mode is superior in its capability to produce strong confinement and relatively low optical loss both at the same time [7–9]. (3) No optical cavity resonance effect is required allowing for broadband operation and ‘athermal’ capability. (4) Lastly, the metal film of the MOS mode can be elegantly used as an electrical contact for modulation, without jeopardizing the optical mode or extra wasted wafer footprint.

Future chip-scale components require a dissipating power consumption as low as 50fJ/bit [18, 19]. With a capacitance of just 7fF for a $5 \mu\text{m}$ long device and an applied bias change of about 4 volts, we can estimate the power consumption per bit to be $E/\text{bit} = \frac{1}{2} CV^2 = 56\text{fJ/bit}$, a value close to the required value. Furthermore, with increasing data bandwidth demands the speed per data channel is being raised as well. In estimating the speed of the device, two factors stand out; (i) the capacitive RC-delay time, and (ii) the formation time of the MOS accumulation layer inside the ITO. Starting with the capacitive effect we find about 300GHz for a realistic resistance of $R = 500 \Omega$ [7] and a $5 \mu\text{m}$ long device. The second effect, can be estimated by calculating the time an electron requires to move across the 10nm thin ITO layer to form the accumulation layer via $\tau = t_{ITO} / v_{drift}$. We estimate the drift velocity via $v_{drift} = \mu E$, where μ is the ITO’s mobility and E the electric field which is proportional to the applied voltage divided by the oxide thickness of the capacitor, $t_{SiO_2} = 20\text{nm}$. The resulting speed is in excess to THz and thus should not be a limiting factor of the device. Notice the drift velocity is about half of the Fermi velocity of ITO [20]. This high performance is possible due to the unique combination of both the MOS-mode and carrier density change of ITO. Notice that the MOS-mode design allows for tunability for modulation strength, power efficiency and operational speed. For instance a doubling of the oxide thickness to 40nm reduces the power dissipation to 23fF/bit , however trading-in modulation depth due to loosened optical confinement.

In conclusion, we have demonstrated a high-performance, Silicon-based, nanophotonic electro-optic modulator. We experimentally demonstrated a 1 dB μm^{-1} extinction ratio with very low insertion losses of about -1 dB for a 3λ -long device and showed broadband operation over a bandwidth of 1000 nm. Furthermore, we verified the modulation mechanism originating from an accumulation layer formed under voltage bias inside the MOS structure resulting in the increase of the imaginary part of the refractive index of the ITO and hence an increased attenuation of the propagating MOS mode. Such a SOI-integrated device with strong modulation strength, low insertion loss and broadband capabilities allows for ultra-compact, power efficient, and potentially fast on-chip data communication links for future photonic integrated circuits [21–23].

Acknowledgments

We acknowledge financial support from the National Science Foundation Nanoscale Science and Engineering Center (NSF-NSEC) under award number CMMI-0751621. We further thank A. Salandrino and H. Suchowski for simulation support and technical support, respectively, and T. Zentgraf for helpful discussions.

Contributions

VJS designed and fabricated the samples, performed optical and electrical measurements, data analysis and theoretical simulations. NDLC performed optical measurements and data analysis. RM proposed the concept and performed data analysis. XZ guided theoretical and experimental investigations. All authors discussed the results and contributed to writing the manuscript.

References

- [1] Miller DAB. Are optical transistors the logical next step? *Nat Photon* 2010;4:3–5.
- [2] Reed GT, Mashanovich G, Gardes FY, Thomson DJ. Silicon optical modulators. *Nat Photon* 2010;4:518–26.
- [3] Liu A, Jones R, Liao L, Samara-Rubio D, Rubin D, Cohen O, Nicolaescu R, Paniccia M. A high-speed silicon optical modulator based on a metal-oxide-semiconductor capacitor. *Nature* 2004;427:615–9.
- [4] Liu M, Bin X, Avila E, Zentgraf T, Ju L, Wang F, Zhang X. A graphene-based broadband optical modulator. *Nature* 2011;474:64–7.
- [5] Bogaerts W, Baets R, Dumon P, Wiaux V, Beckx S, Taillaert D, Luyssaert B, Van Campenhout J, Bienstman P, Van Thourhout D. Nanophotonic waveguides in silicon-on-insulator fabricated with CMOS technology. *J Lightwave Technol* 2005;23(1):401–12.
- [6] Xu Q, Schmidt B, Pradhan S, Lipson M. Micrometre-scale silicon electro-optic modulator. *Nature* 2005;435:325–7.
- [7] Oulton RF, Sorger VJ, Pile DFB, Genov D, Zhang X. Nanophotonic confinement and transport in a hybrid semiconductor-surface plasmon waveguide. *Nat Photon* 2008;2:496–500.
- [8] Sorger VJ, Ye Z, Oulton RF, Bartal G, Wang Y, Zhang X. Experimental demonstration of low-loss optical waveguiding at deep sub-wavelength scales. *Nat Commun* 2011;2:331.
- [9] Sorger VJ, Pholchai N, Cubukcu E, Oulton RF, Kolchin P, Borschel C, Gnauck M, Ronning C, Xiang X. Strongly enhanced molecular fluorescence inside a nanoscale waveguide gap. *Nano Lett* 2011;11(11):4907–11.
- [10] Dionne JA, Diest K, Sweatlock LA, Atwater HA. PlasMOSstor: a metal-Ox-Si field effect plasmonic modulator. *Nano Lett* 2009;9(2):897–902.
- [11] Cai W, White JS, Brongersma ML. Compact, high-speed and power-efficient electrooptic plasmonic modulators. *Nano Lett* 2009;9(12):4403–11.
- [12] Gordon RG, Bulletin MRS. Criteria for choosing transparent conductors. *MRS Bulletin* 2000;25(8):52–7.
- [13] Hamberg I, Granqvist CG. Evaporated Sn-doped In_2O_3 films: basic optical properties and applications to energy-efficient windows. *J Appl Phys* 2000;123–59.
- [14] Feigenbaum E, Diest K, Atwater HA. Unity-Order index change in transparent conducting oxides at visible frequencies. *Nano Lett* 2010;10(6):2111–6.
- [15] Melikyan A, Lindenmann N, Walheim S, Leufke PM, Ulrich S, Ye J, Vincze P, Hahn H, Schimmel Th, Koos C, Freude W, Leuthold J. Surface plasmon polariton absorption modulator. *Optics Express* 2011;19(9):8855–69.
- [16] Michelotti F, Dominici L, Descrovi E, Danz N, Menchini F. Thickness dependence of surface plasmon polariton dispersion in transparent conducting oxide films at 1.55 μm . *Optics Lett* 2009;34(6):839–41.
- [17] Kaminow IP, Doerr CR, Dragone C, Koch T, Koren U, Saleh AAM, Kirby AJ, Ozveren CM, Schofield B, Thomas RE, Barry RA, Castagnozzi DM, Chan VWS, Hemenway BR Jr, Marquis D, Parikh SA, Stevens ML, Swanson EA, Finn SG, Gallager RG. *IEEE J Select Top Commun* 1996;14:780–99.
- [18] Miller DAB. Physical reasons for optical interconnection. *Int J Optoelectron* 1997;11:155–68.
- [19] Miller DAB. Device requirements for optical interconnects to silicon chips. *Proc IEEE* 2009;97(7):1166–85.
- [20] Loque A, Hegedus S. *Handbook of photovoltaic science and engineering*, 2nd edn. John Wiley and Sons; 2001: p. 733.
- [21] Paniccia M. Integrating silicon photonics. *Nat Photon* 2010;4:498–9.
- [22] Liao L, Liu A, Rubin D, Basak J, Chetrit Y, Nguyen H, Cohen R, Izhaky N, Paniccia M. 40 Gbit/s silicon optical modulator for high-speed applications. *Electron Lett* 2007;43(22):1196–7.
- [23] Kirchain R, Kimerling L. A roadmap for nanophotonics. *Nat Photon* 2007;1:303–5.

Received February 26, 2012; accepted April 9, 2012